JOURNAL OF CATALYSIS 31, 173–199 (1973)

Activity of Nickel Catalysts for Steam Reforming of Hydrocarbons

JENS R. ROSTRUP-NIELSEN

Haldor Topsøe A/S, P.O. Box 49, DK-2860 Søborg, Denmark

Received March 7, 1973

A number of catalysts have been investigated to identify some factors of chemical composition and surface structure which may influence the activity for steam reforming of hydrocarbons. The kinetics for ethane reforming at 500°C are influenced by the composition of the catalyst. The specific activity is very low on some support materials, and when alkali is present. The activity correlates with the surface heterogeneity expressed by adsorption of nitrogen on the nickel surface. The activity trend observed for reforming of ethane is generally following that obtained for reforming of other hydrocarbons, hydrogenolysis of ethane, and methanation of carbon monoxide; whereas decomposition of ammonia appears unaffected by the carrier or the presence of alkali. Various explanations for the effect of the carrier and of alkali are discussed.

In many kinetic studies of chemical processes a single catalyst sample is investigated in great detail to provide a basis for calculation of the catalyst volume required for a given conversion in industrial reactors. Tubular steam reforming of higher hydrocarbons is a process where secondary effects of catalyst activity may have an influence comparable to that on the overall conversion. Steam reforming of higher hydrocarbons is a complex process including several consecutive and parallel reactions of which some may result in coke. The overall reaction can be described by the breakdown of the hydrocarbon:

$$C_nH_m + nH_2O \rightarrow nCO + \left(n + \frac{m}{2}\right) H_2 \quad (1)$$

followed by establishment of the equilibria:

$$CO + H_2O = CO_2 + H_2, \quad (2)$$

$$CO + 3H_2 = CH_4 + H_2O. \quad (3)$$

Tubular reformers are working normally at catalyst inlet and exit temperatures in the ranges 450–550 and 650–850°C, respectively. The catalyst activity determines the minimum exit temperature to be applied without breakthrough of higher hydrocarbons. This may be a problem in reformers for towns gas production (*1*, *2*). In most reformers for production of synthesis gas and hydrogen, the composition of the exit gas will be very close to the equilibria of reactions (2) and (3) established at the exit temperature and, normally, design restrictions to ensure long tube lives will determine the maximum throughput.

High catalyst activity may result in lower tube wall temperatures. In addition, it may imply reduced risks of coking because the breakdown of the higher hydrocarbons may be completed in the colder part of the bed where coking rates are smaller (*1*, *3*). However, this study deals only with the activity for conversion of the higher hydrocarbons, reaction (1), whereas the selectivity problems will be reported later. Moreover, the rates of the simultaneous reactions, (2) and (3), have not been considered and no attempts have been made to evaluate a complete kinetic expression to be applied in reactor design. As shown in Table 1 very different results have been reported on the kinetics of reaction (1) (*4–8*). Balashova, Slovokhotova and Balandin (*4*) observed the reaction order with

TABLE 1
RESULTS FROM SOME KINETIC STUDIES OF STEAM REFORMING OF HIGHER HYDROCARBONS

Authors	Catalyst system	Hydrocarbon	Temp (°C)	Pressure (atm abs)	Kinetic coefficients $\alpha_{C_nH_m}$	Kinetic coefficients α_{H_2O}	Activation energy (kcal/mol)
Balashova, Slovokhotova and Balandin (4)	Ni/SiO_2 Ni/C	Cyclohexane	400–460	(1)	0 No activity	0–1	22–24
Bhatta and Dixon (5)	Ni/γ-Al_2O_3	*n*-Butane	425–475	30	0	1	
Bhatta and Dixon (6)	Ni/γ-Al_2O_3	*n*-Butane		30	0	1	13
	Ni/α-$Al_2O_3UO_2$ (0.3% *K*)		404–491	30	1	−0.6	24
Phillips, Mulhall and Turner (7)	Ni/γ-Al_2O_3	*n*-Hexane *n*-Heptane	360–450	15	0.3	0–0.07	21
Saito *et al.* (8)	Ni/SiO_2	*n*-Butane	370–450	1	0	1	

respect to steam to vary with the range of steam partial pressure, and the data of Bhatta and Dixon (6) demonstrated that the kinetics may change significantly from catalyst to catalyst.

The purpose of the present work has been to identify some of the factors in chemical composition and surface structure of the catalyst which may influence the activity. Various catalyst preparations have been investigated but a more detailed kinetic study has only been made with a single catalyst sample. The study has been limited to temperatures around 500°C, a typical inlet temperature of the catalyst bed, because a high activity for reaction (1) is assumed to be important in this part of the bed. The activity has been estimated mainly from isothermal steam reforming experiments at atmospheric pressure. Ethane, being the simplest higher hydrocarbon, was selected as feed. Some experiments have been performed at pressure using various pure hydrocarbons and naphtha as feed. Finally, the activities for other reactions, methane reforming, methanation, decomposition of ammonia and ethane hydrogenolysis, have been estimated for some of the catalysts from experiments at atmospheric pressure. The activity tests have been supplemented by chemisorption studies.

METHODS

1. *Ethane Reforming at Atmospheric Pressure*

Apparatus. The experiments were performed in a simple flow system with a

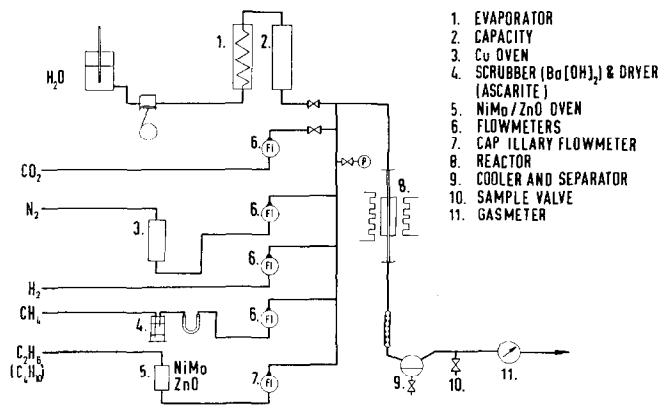

FIG 1. Apparatus for studies of ethane reforming and other reactions at atmospheric pressure.

tubular fixed bed reactor as shown in Fig. 1. The reactor, which was made of 18/8 stainless steel, was surrounded by an electrically heated furnace. A metal block with an external diameter of 25 mm was mounted on the reactor to ensure isothermal conditions. The internal diameter of the reactor was 5.04 mm, and a thermowell with external diameter of 2.0 mm was placed in the axis of the reactor. The temperature of the catalyst bed was adjusted by means of a thyristor controller. The axial temperature gradient is estimated to be less than 1°C/cm in the catalyst bed.

The gas flows were controlled by flowmeters, whereas the addition of H_2O was followed on a buret.

Gases. All gases except H_2 were taken from cylinders. H_2 (impurities (mainly O_2) less than 0.03%) was made in an Oerlikon electrolyzer and used without further purification. C_2H_6 was purified over NiMo catalyst and ZnO at 270°C. Gas chromatographic analyses showed impurities of CH_4 (max 0.01 vol %), C_2H_4 (0.04–0.66 vol %), C_3H_8 (0.02–0.08), and C_3H_6 (0.02–0.40 vol %). N_2 was purified over Cu wire at 250–275°C. CO_2 was used without purification.

Procedure. A sample of 0.1–0.4 g of reduced catalyst as 0.3–0.5 mm particles was placed in the reactor. The catalyst was heated in H_2 (0.18 mol/hr) to the temperature to be used for the experiment (normally 500°C) and steam was added. After condensate was observed in the cooler and steam flow checked by sampling of condensate, ethane and, in a few experiments, also CO_2 were added. All experiments were performed with H_2 in the feed (H_2O/H_2 = approx 10) to avoid oxidation of the catalyst. When the exit gas flow was stabilized a sample of the dry exit gas was taken, and the conditions were changed. Normally, the activity stabilized within less than 30 min. However, over periods of days a gradual deactivation was observed which could be ascribed to sulfur poisoning. Owing to this the bed was changed after each run, normally having a maximum duration of approx 6 hr. In a few cases the bed was used for two runs. The parameter to be changed during the run was varied unsystematically with time to minimize the influence of poisoning. Moreover, as a check each experiment was completed at the same conditions as the starting conditions. After each experiment the weight of the catalyst was checked.

The gas sample was analyzed by means of Orsat (CO_2) and gas chromatographic analysis. At the normal conditions the main products were CO_2 and H_2.

Evaluation. The reaction of ethane with steam:

$$C_2H_6 + 4H_2O = 2CO_2 + 7H_2, \qquad (4)$$

can be considered irreversible as K_p (500°C) = 155 atm[4].

For simplicity a kinetic expression of the power form was selected:

$$r = F\frac{dx}{dw} = Ae^{-E_a/RT}\prod_i p_i^{\alpha_i}, \qquad (5)$$

where $F = C_2H_6$ inlet flow, W = catalyst weight, and x = conversion. The conversion of C_2H_6 was calculated on basis of the exit gas analysis by:

$$x = \frac{(CH_4) + (CO) + (CO_2)}{(CH_4) + (CO) + (CO_2) + 2(C_2H_6)} \times 100\%. \qquad (6)$$

The kinetic parameters were estimated from plots of the conversion and the parameter in question, and the estimated values were used for computer integrations of (5) assuming no diffusion restrictions and no temperature gradients. On the basis of the calculated rate constants the kinetic parameters were changed until the variance was minimized. In the calculations the measured H_2O addition was used as the H_2O-feed, whereas the inlet gas flows were calculated on the basis of the exit gas analysis and the measurement of the exit gas flow. This procedure was found to be more accurate than using the readings of the flowmeters. The mass balance of the apparatus was checked in a few experiments where gas samples were taken before and after the reactor. Relative deviations in ethane contents of less than 1% were indicated. Blank experiments at 500°C with alumina particles showed no conversion.

The calculation procedure described could not be applied in experiments with C_2H_6 and CO_2 in the feed, and in all these experiments gas samples were taken before and after the reactor. The inlet gas flows of CO_2 and C_2H_6 were calculated from the CO_2/C_2H_6 ratio of the feedgas, the exit gas analysis and the exit flow. The conversion was calculated from the ethane mass balance.

In order to compare the activities of catalysts with different kinetic parameters the initial rate r_i was calculated at following standard conditions: $H_2O/C_2H_6 = 8$; $H_2O/H_2 = 10$; temperature = 500°C; and pressure = 1.0 atm abs.

2. Other Reactions Tested at Atmospheric Pressure

The apparatus used for ethane reforming experiments was also used for experiments on methane reforming, ammonia decomposition, and ethane hydrogenolysis. CH_4 and NH_3 were taken from cylinders. CH_4 containing less than 0.02% of higher hydrocarbons was purified by washing in a $Ba(OH)_2$ solution and over ascarite to remove an impurity of CO_2 (0.7 vol %). NH_3 was used unpurified.

The methane reforming experiments were evaluated in a similar way as the ethane reforming experiments assuming first order kinetics with respect to methane as generally agreed in the literature (*9*, *10*):

$$r = k \cdot p_{CH_4}(1 - Q/K_p), \qquad (7)$$

where Q and K_p are reaction quotient and equilibrium constant for:

$$CH_4 + 2H_2O = CO_2 + 4H_2. \qquad (8)$$

The activities were compared by the initial rates calculated at the same standard conditions as above with $H_2O/CH_4 = 4$.

In the experiments on decomposition of ammonia:

$$2NH_3 = N_2 + 3H_2, \qquad (9)$$

the unconverted ammonia was absorbed in a solution of sulfuric acid and the conversion was calculated from the amount of washed exit gas and the ammonia feed. The activity was expressed as the conversion at 500°C using a space velocity of 9.0 mol NH_3/g cat/hr.

The experiments on ethane hydrogenolysis:

$$C_2H_6 + H_2 = 2CH_4, \qquad (10)$$

were performed with following feed:

C_2H_6	5 vol%
H_2	20 vol%
N_2	75 vol%.

Reaction (10) is generally reported to be first order with respect to C_2H_6 (*11*), whereas the order with respect to H_2 may vary. However, the partial pressure of H_2 can be considered as constant due to the large excess and the conversions being less than 10%. Therefore, the activity was expressed as the first order rate constant at 300°C.

The methanation experiments were performed in the apparatus used and described by Schoubye (*12*). A mixture of H_2 containing approx 1 vol % CO was used as feed (0.1 Nm^3/hr). The reaction:

$$CO + 3H_2 = CH_4 + H_2O, \qquad (11)$$

was performed isothermally at a temperature in the range 200–300°C depending on the expected activity. The catalyst was used as 0.4–0.5 mm particles in amounts of 0.5 g. The initial rate was calculated on the basis of the kinetics of Schoubye (*12*) at the following standard conditions: 1 vol % CO in H_2; temperature = 250°C; pressure = 1.0 atm abs.

3. Reforming Experiments at Elevated Pressure

Apparatus. The apparatus was designed to simulate operation under industrial conditions. Water and liquid hydrocarbon feed were pumped to an evaporator and mixed with gaseous hydrocarbons and N_2 to be used as feed. The feed mixture was passed through a vessel for mixing and a preheater to a tubular reactor. H_2 was added just before the reactor. The reactor effluent was depressurized and passed through a cooler and a separator to a gas meter.

The reactor was made of 18/8 stainless steel and had an internal and external diameter of 10.0 and 17.5 mm, respectively. One thermowell with external diameter 3 mm was placed in the axis of the reactor, and another at the external surface. The reactor was surrounded by an electrically heated furnace with 3 independent sections. The heated length of the reactor was 60 cm, whereas the height of the catalyst bed was 10 cm. The catalyst zone consisted of 0.25—approx 10 g of catalyst as 1–2 mm particles diluted to constant volume with particles of magnesium aluminum spinel. The amount of catalyst was determined such that conversions and temperature gradients were of the same order of size in all experiments. Above the catalyst zone was placed a layer of 5 cm of particles of magnesium aluminum spinel. The temperature was adjusted by thyristor controllers, and the pressure was maintained by a pneumatic control valve. The flows of water and liquid hydrocarbons were indicated on burets, whereas the gas feeds were measured on flowmeters. The axial temperature gradient in the catalyst bed was found to be approx 1°C/cm, whereas the temperature difference between the external tube wall and the axis of the bed varied between 2 and 10°C. On this basis the experiments cannot be considered as strictly isothermal, and the results may only be used for relative comparisons of the catalysts.

Feedstock. The compositions of the feedstocks were determined by gas chromatographic analysis. The liquid hydrocarbons were desulfurized in a separate apparatus over NiMo catalyst and ZnO. Analyses showed contents less than 0.05 ppm S. The gaseous hydrocarbons, N_2 and H_2 were used unpurified.

Procedure. Before each experiment the apparatus was checked for leakages in H_2 at 36 atm abs. The reactor was heated up in H_2 to about 400°C. Steam and then gradually hydrocarbon feed were added and the process conditions were established. All experiments were performed with addition of H_2, ($H_2O/H_2 = 10$), to avoid oxidation. It soon turned out that the catalyst activity could not be maintained for more than a few hours. This could be ascribed to sulfur poisoning caused by the quick accumulation of sulfur at the extremely high throughputs. Therefore, most of the experiments included only one measurement. As standard conditions were used:

Pressure	31 atm abs
Mean temp	500°C
H_2O/C	4 mol/atom
H_2O/H_2	10 mol/atom

In a few experiments where the total pressure was changed, this was done in an unsystematic way to minimize the influence of poisoning. Samples of dry exit gas and in some cases a sample of unconverted hydrocarbon were taken and analyzed by means of a gas chromatograph and Orsat analysis (CO_2).

Evaluation. The conversion, x, of the higher hydrocarbons was calculated from the analysis and flow measurement of the exit gas giving the g atoms of CO, CO_2 and CH_4 formed, and from the measured consumption of liquid hydrocarbon giving the total g atoms of C in the feed. In the experiments with gaseous feed the conversion was calculated on basis of the exit gas only. Assuming pseudo-first order kinetics with respect to the hydrocarbon an apparent constant k_a was calculated from:

$$k_a = \frac{F}{W} \ln\left(\frac{1}{1-x}\right). \qquad (12)$$

In an experiment with CH_4 as feed, x was replaced by x/x_{eq} where x_{eq} is the conversion to establish the equilibrium. As described by Hougen and Watson (*13*) for situations where the kinetic expression is unknown, it may be useful for comparing different catalysts to assume that even complex catalytic systems approximate to a pseudo-first order relationship if only space velocity is varied. However, it must be emphasized that the apparent rate constant obtained by this empirical method may hardly be used for prediction of catalyst performance at other conditions. It should be used only for relative comparison

TABLE 2
PROPERTIES OF CATALYSTS: A-TYPES

Catalyst no.	Comments	Na (wt %)	Contents of red. Ni (wt %)	Ni area (m^2/g)	Total area (BET) (m^2/g)	n_0 N_2-capacity (B_5) (N cm^3/kg)	Particle size: Calc. r_{mean} (Å)	Particle size: Electron microscope particle ϕ (Å)	Activity for C_2H_6 reforming 500°C: r_i (mol/g/hr × 10)	Activity for C_2H_6 reforming 500°C: r_s (mol/m^2 Ni/hr × 10^3)
Group 1. Fixed composition (25 wt % Ni). Na: 0.04–0.16 wt %. Preparation route 1.										
A1		0.07	23.8	2.00	20.0	14	398	250–2500	2.4	120
A15		0.04	22.0	3.01		34	245		4.40	145
A3		0.05	16.4	6.97	45.5	172	79	50–250	8.25	118
A4		0.05	23.1	3.78	33.3	5	205	500–1000	2.0	53
A16		0.14	22.9	2.99			257		1.5	52
A7	A16 sintered	0.16	23.5	1.06			740	150–2000	0.51	48
A17		0.10	26.4	2.72		80	326		1.4	52
A18		0.08	25.7	3.46	27.4	50	249		4.2	122
Group 2. Fixed composition (25 wt % Ni). Na < 0.01 wt %. Various preparation routes.										
A19	A1 washed in H_2O					108			4.0	198
A20	Preparation route 2		18.1	3.71	15.7	112	163		8.2	222
A21	A20 sintered		10.1	1.09	2.34		311		2.0	183
A22	Preparation route 1		20.0	4.16	25.1	79	161		11.9	287
A23	A22 sintered		22.9	1.08	8.6	5	684		2.9	282
A24	Preparation route 1		20.4	8.87	53.7		77		20.4	230
A25	Preparation route 3		20.3	6.34	39.8	179	107		10.5	165

Group 3. Ni content varied. Na < 0.01 wt %. Preparation route 1.										
A10	Ni/Mg = 1/1	0.04	13.9	4.17		96	112	50–125	10.6	254
A26	0.25/1		4.3	2.12			68	75–200	1.9	90
A27	0.5/1		8.2	4.35			63	75–200	9.5	212
A28	1/1		14.2	6.10			78	75–200	18.4	299
A29	2/1		23.9	8.50			94	75–300	16.8	197
A30	4/1		35.1	8.45			139	200–600	18.6	221
A31	6/1		41.9	3.64			385	500–1000	8.0	219
A32	8/1		48.3	3.35			485	2000–5000	7.1	214
Group 4. Other metals (total content of metals 25 wt %) Na < 0.01 wt %. Preparation route 1.										
A13	Ni/Cu = 0.7/1.3		7.6	(1.23)				50–150	0.020	1.6
A14	Ni replaced by Co		22.9[a]	5.48			140	(500)	0.016	0.29
A33	Ni/Co = 3/1		25.0[a]	6.34			132		2.9	46
Group 5. Promoted with alkali (25 wt % Ni)										
A34	Al 0.14 wt % K[b]			2.95					0.79	27
A35	Al 0.53 wt % K[b]			2.65					0.097	3.7
A36	A25 2.1 wt % K[c]			3.58	43.5	70	107		0.075	2.1
A37	Al 0.61 wt % Na[b]			2.44					0.32	13
A38	A24 0.11 wt % Na[b]								13.4	151
A39	A24 0.46 wt % Na[b]								7.2	81
A40	A24 0.78 wt % Na[b]								7.6	86

[a] Red. Co or Co + Ni.
[b] Alkali added after reduction.
[c] Alkali added during preparation.

TABLE 3
PROPERTIES OF CATALYSTS: B–E TYPES

Catalyst type	Support material	Comments	Contents of red. Ni (wt %)	Ni area (m^2/g)	Total area (BET) (m^2/g)	n_0 N_2 capacity (B_5) (ml/kg)	Particle size: Calc r_{mean} (Å)	Particle size: Electron microscope particle ϕ (Å)	Activity for C_2H_6 reforming 500°C: r_i (mol/g/hr × 10)	Activity for C_2H_6 reforming 500°C: r_s (mol/m^2 Ni/hr × 10^3)
Type B. Based on $MgAl_2O_4$										
B1	$MgAl_2O_4$		8.0	0.44	4.19	12	607	500–2500	1.6	366
B5	$MgAl_2O_4$	1.57 wt % K[a]	11.1	1.35			272		0.029	2.1
B6	$MgAl_2O_4$	0.52 wt % K[a]	17.0						0.54	61
B4	$MgAl_2O_4$	1.53 wt % K[a]	17.5	0.88			664		0.074	8.3
Type C. Based on Al_2O_3										
C1	η-Al_2O_3		16.5	7.01		65	79	100–400	5.5	80
C6	η-Al_2O_3 Cl	1.7 wt % K[b]		6.34		29			1.8	29
C7	η-Al_2O_3 Cl	5.8 wt % K[b]		3.89		0.5			0.45	11
C8	η-Al_2O_3 Cl	1.3 wt % Na[b]		6.78		13			3.2	47
C9	η-Al_2O_3 Cl	1.1 wt % Ca[b]		7.24		115			2.2	30
C2	γ-Al_2O_3		17.9	5.66	106	238	106		9.2	163
C3	γ-Al_2O_3		20	3.62	71.1	196	185		8.2	227
C10	γ-Al_2O_3 C3	2.1 wt % K[a]		4.19	76.4	13	160		1.9	46
C4	γ-Al_2O_3	red. at 500°C	44.3	11.31		586	131		34.3	304
C5	α-Al_2O_3		6.3	1.39			121		2.0	141
Type D. Based on various materials										
D2	MgO		5.3	1.61			146		4.3	266
D3	MgO, Al_2O_3, ($MgAl_2O_4$) Mg/Al = 0.5		19.1	14.5			44		17.4	120
D4	ZrO_2		16.2	2.58		0.5	210		0.067	2.6

D5	ZrO_2/γ-Al_2O_3	Zr/Al = 0.44	25.0	5.70			147		11.5	201
D6	Cr_2O_3	red. at 500°C	60.0	7.92			254		19.9	252
D8	SiO_2		21.2	12.67	145		53		16.8	133
D9	SiO_2/Al_2O_3	Si/Al = 3	21.2	4.43		382	76		1.1	25
D10	SiO_2/Al_2O_3	Si/Al = 2.1 3.9% Na[a]	25	2.45	44		336		0.44	18
D11	SiO_2/MgO	Si/Mg = 1.67	25	2.42	33		346		0.58	24
D12	D11 with 0.49 wt % K[a]		25	2.13	10		394		0.097	4.5
D13	TiO_2		37.0	1.00			125		0.36	36
D14	Carbon[c]		14.4	(0.8)				500–1700	0.040	5
D7	Cr_2O_3	red. at 500°C	12.3	5.43			76		14.1	260
Type E. Containing precious metals										
E1	Al_2O_3	Pt	0.5[e]	0.24[e]					0.53	221
E2	Al_2O_3	Pt	5.0	1.54					1.2	77
E3	carbon[d]	Pt	0.5	0.55						
E4	Al_2O_3	Pd	0.5	0.41					0.87	212
E5	Al_2O_3	Pd	5.0	3.46					6.7	180
E6	γ-Al_2O_3	Pd		0.10					0.19	194
E7	carbon	Pd	0.5	0.20						
E8	Al_2O_3	Ru	0.5	0.26					5.4	2059
E9	Al_2O_3	Ru	5.0	1.81					30.3	1673
E10	γ-Al_2O_3	Ru		0.55					0.20	37
E11	carbon[d]	Ru	0.5	0.48						
E12	γ-Al_2O_3	Rh		0.17					4.1	2502
E13	carbon[d]	Rh	0.5	0.37						
E14	γ-Al_2O_3	Re		0.21					0.10	50

[a] Added during preparation.
[b] Added before reduction.
[c] Ni area estimated from particle diameter.
[d] Diluted with γ-Al_2O_3, 1/10.
[e] Following figures based on metals indicated.

of catalyst activities or reactivities of various hydrocarbons.

4. Catalysts

The catalysts which are listed in Tables 2 and 3 have been divided into various types determined by their chemical compositions. The A-type is based on magnesia containing approx 6 wt % Al. Group 1 has a minor content of Na (0.02–0.16 wt %) whereas groups 2–4 are free of alkali metals (less than 0.01 wt %). Group 2 includes catalysts with fixed composition but with different preparation routes whereas the Ni content is varied in group 3. The B-type is based on magnesium aluminum spinel whereas the C-type is supported by various types of alumina. Catalysts based on other supports are represented by Type D and, finally, type E covers catalysts containing precious metals. If not indicated in the tables the catalysts of groups B–E contain no alkali metals (less than 0.01 wt %). The numbering of the catalysts is made in accordance with the numbering used previously (*14*). Some of the catalysts were prepared in parallel and may present a better basis for comparisons. In addition to what is indicated in Tables 2 and 3 such groups are (A20–A23), (A26–A32), (B1 and B4–B6), and (A25, A36, C7, C8, D8, D10 and D11).

The catalysts were reduced in a separate reactor at 850°C in H_2 for a period of 2 hr unless otherwise indicated. The content of nickel in the reduced state was determined as previously (*14*). The nickel surface area was calculated on basis of the sulfur capacity assuming the saturated surface to contain 44.2×10^{-9} g S/cm^2. The sulfur capacity was determined by chemisorption of H_2S at 500°C as described previously (*15*). A mean particle radius was calculated from the nickel surface area and the content of reduced nickel as shown earlier (*14*). This figure should be used only as an indication. For some catalysts the range of nickel particle size was estimated by means of an electron microscope. A N_2 capacity of the Ni surface was determined by a procedure described below.

5. Adsorption Studies

The presence of special sites on the nickel surface was investigated on basis of the work by Van Hardeveld *et al.* (*16–19*) who found that N_2 was physisorbed on the so-called B_5-sites of nickel crystallites in the range 15–70 Å in a polarized state which was infrared active. The polarization explains the relatively high initial heat of adsorption (approx 13 kcal/mol). Other studies (*20–22*) have considered the IR active N_2 as weakly chemisorbed molecules, whereas the results of Bradshaw and Pritchard (*23*, *24*) appear consistent with those of Van Hardeveld *et al.*

As demonstrated by Van Hardeveld and Van Montfort (*19*) the determination of the number of B_5-sites either by IR or volumetric methods is not unambiguous, as there is no simple correlation between the intensity of the IR-absorption band of the adsorbed N_2 and the number of B_5-sites. The results make it likely that all N_2 adsorbed at room temperature and relatively low pressure is adsorbed in the IR-active form, but this N_2 is only a fraction of that which can be adsorbed at higher pressure or lower temperature. On this basis Van Hardeveld (*25*) has proposed measurement of the adsorbed volume at room temperature and a N_2 pressure of 200 mm Hg as a standard method for determination of the number of B_5-sites.

This method has been adopted here, and as a correction for ordinary physically adsorbed N_2, the measurement was repeated after poisoning the nickel surface with N_2O. The N_2 capacity, n_9, was determined as the difference between the two adsorbed volumes at 200 mm Hg. The measurements were performed in a conventional BET apparatus as described previously (*15*). A sample of 15–20 g of prereduced catalyst was heated in a flow of H_2 and evacuated for approx 3 hr at 800°C to a pressure below 10^{-4} mm Hg before the measurements. The high evacuation temperature was necessary to remove all H_2 from the surface. It was evident that H_2 could still be removed when heating the evacuated sample from 600 to 800°C. Evacuation at

600°C only resulted in smaller values of the N_2 capacity. Catalyst C4 was reduced in the equipment at 500°C but evacuated at 800°C.

Some isotherms are shown in Fig. 2. For catalyst C4, which was the catalyst with the highest N_2 capacity, the contribution from the physically adsorbed N_2 is negligible, whereas the N_2 capacity of a typical catalyst like A1 is determined as the difference between two figures of same order. This makes the determination of n_0 very uncertain. Even catalyst C4 shows a value of n_0 of approximately one order of magnitude less than the typical values of the catalyst of Van Hardeveld. This is explained by the larger nickel crystallites of the present catalysts. The high uncertainty of the small adsorption volumes makes an estimation of the initial heat of adsorption very unsafe. On basis of the isotherms on C4 at 25 and 65°C an initial isosteric heat of adsorption was estimated to about 11 kcal/mol N_2.

Results

1. *Ethane Reforming*

A series of experiments was performed to determine a kinetic expression for ethane reforming at 500°C over catalyst A1. Minimum variance for an expression of the form (5) was obtained by:

$$r = 1.67 \times 10^5 \, e^{-18100/RT} p_{C_2H_6}^{0.54} p_{H_2O}^{-0.33} p_{H_2}^{0.2} \text{ mol/g} \cdot \text{hr.} \quad (13)$$

The effect of the partial pressure of carbon dioxide appeared insignificant. Experiments at 450 and 550°C including variations of the partial pressure of steam showed $\alpha_{H_2O} = -0.60$ and -0.23, indicating that a more complex expression is required to describe the kinetics of the reaction in a broad temperature range. In this connection it should be noticed that Bodrov, Apel'baum and Temkin (*9*) found the kinetic coefficient of hydrogen to vary with temperature in their studies of the methane reforming reaction.

The kinetic coefficients, mainly for steam, were determined for some other catalysts. As shown in Table 4 the reaction order with respect to steam varied significantly from catalyst to catalyst. Thus, catalysts containing free magnesia (A-types and D3) showed negative values of α_{H_2O} down to -0.5, whereas catalysts based on magnesium aluminum spinel (B1) or alumina (C1) showed values of zero or slightly positive, respectively. The addition of potassium caused a significant decrease of α_{H_2O}. The addition of sodium had a less pronounced effect. The addition of potassium implied no change of the apparent activation energy whereas replacement of nickel with a nickel–copper alloy caused a substantial increase of the activation energy. This is demonstrated in Fig. 3.

The influence on the experiments of mass and heat transfer was analyzed by means of the Topsøe REACTOR program (*26*) designed for computer calculation of the temperature and conversion profiles of a fixed bed converter. The calculation is performed on the basis of the intrinsic kinetics and the pore volume distribution of the catalyst. For catalyst A18, a catalyst at a typical activity level, the calculation showed an effectiveness factor of more than 0.95 and a temperature drop over the gas film surrounding the particles of 1.3°C, which reflects only negligible restrictions. For a very active catalyst such as A22,

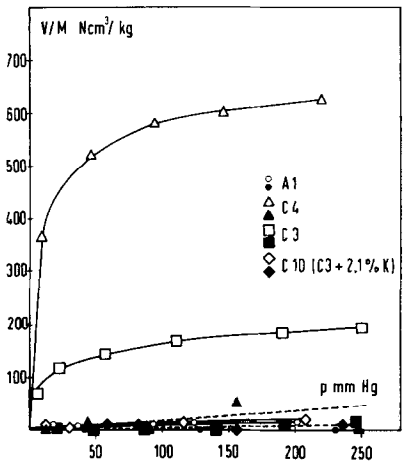

FIG. 2. Isotherms for N_2-adsorption at 25°C. Measurements after passivation of Ni surface with N_2O indicated by filled points and broken lines.

TABLE 4
ETHANE REFORMING AT ATMOSPHERIC PRESSURE, 500°C: SUMMARY OF KINETIC PARAMETERS[f]

Catalyst type	Comments	Kinetic coefficients C_2H_6	H_2O	H_2	Apparent activation energy E_a, (kcal/mol)	
Type A, Group 1 (MgO)						
A1		0.54[a]	−0.33[a]	0.2[a]	18.1	(0.15)
A18			−0.52[b]			
	Group 2					
A19			0.0			
A21			−0.26[c]			
A22			−0.48[c]			
A23			−0.17[c]			
A13					24.4	(0.7)
	Group 5 (Promoted)					
A34	Al, 0.14 wt % K		−0.42[c]		18.9	(0.3)
A35	Al, 0.53 wt % K		−1.81[e]		19.6	(0.5)
A37	Al, 0.61 wt % Na		−0.7			
Type B, ($MgAl_2O_4$)						
B1			0.0[b]		18.3	(2.5)
B4	1.53 wt % K	(0.4)[c]	−1.08[d]			
Type C, (Al_2O_3)						
C1		(0.6)[c]	0.13[a]			
Type D						
D3	MgO/Al_2O_3 = 1/1		−0.26[b]			
D4	ZrO_2				19.2	(0.9)

[f] Figures in brackets indicate the accuracies of the activation energies. The accuracies of the coefficients are estimated to: [a] ≤0.05; [b] 0.05–0.1; [c] 0.1–0.2; [d] 0.2–0.3; [e] 0.3–0.5.

some transport restrictions were indicated by an effectiveness factor of approx 0.9 and a temperature drop over the gas film of 4–5°C.

Due to the variations in kinetic coefficients from catalyst to catalyst the activities were compared on the basis of initial rates r_i as described previously. For catalysts for which no kinetic coefficients were determined, r_i was calculated on the basis of the kinetics of a similar catalyst. The relative standard deviations of r_i calculated from experiments based on samples of the same origin and of the corresponding nickel areas were estimated to be approx 17 and 10%, respectively, which yield a relative standard deviation of the specific rate r_s of no better than 20%. Therefore, the experiments only allow identification of substantial differences of specific activity.

From the results shown in Tables 2 and 3 the alkali-free nickel catalysts appear to have a specific activity in the range r_s = 0.1–0.35 mol/m² Ni/hr. This is observed on a broad range of support materials such as magnesia in various sintered forms, and with Al/Mg ratios varying from 0 to 2, magnesium aluminum spinel, alumina in different modifications, alumina stabilized by zirconia, chromia and silica. Moreover, results from a systematic series of catalysts (A22–A32) shown in Fig. 4 indicate only insignificant influence on the specific activity of the nickel content and of the nickel crystallite size varying with the nickel content from 50 to 5000 Å. The results might reflect less specific activity on the smallest crystallites but more experiments with catalysts with nickel crystallites below 70 Å are required to elucidate this effect.

Some alkali-free catalysts show a small

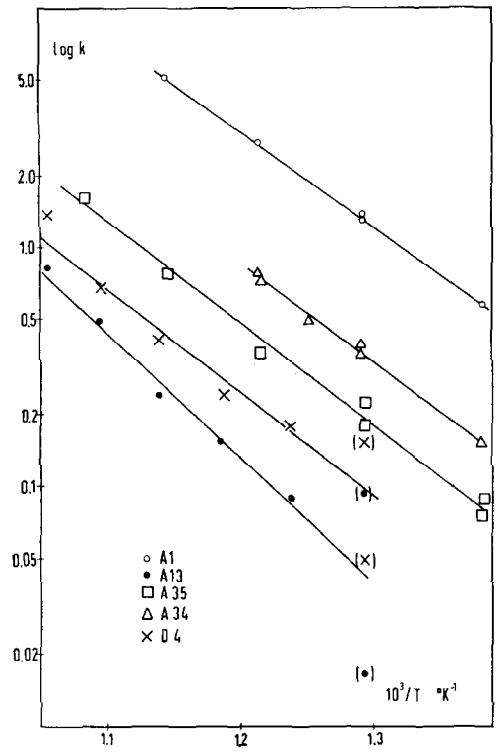

FIG. 3. Temperature dependence of rate constant for ethane reforming at 500°C.

specific activity. The catalysts based on silica–alumina, silica–magnesia and on titania had $r_s = 0.02$–0.04 mol/m² Ni/g, whereas the activity of catalysts based on pure zirconia and carbon was very poor with $r_s = 2.6 \times 10^{-3}$ and 3.8×10^{-4}, respectively. The low activity of the zirconia based catalyst (D4) is not accompanied by an activation energy differing from that of catalyst A1. The activity of the zirconia–alumina based catalyst (D5) appears normal, which may be explained by nickel being supported mainly by alumina as it was present as nickel aluminum spinel before the reduction.

The addition of potassium to the catalysts can result in a decrease of the specific activity of more than one order of magnitude. This is demonstrated in Fig. 5 which indicated the influence to be stronger on A- and B-types than on C-types. The effect of sodium addition is less than that of potassium. The significant influence of po-

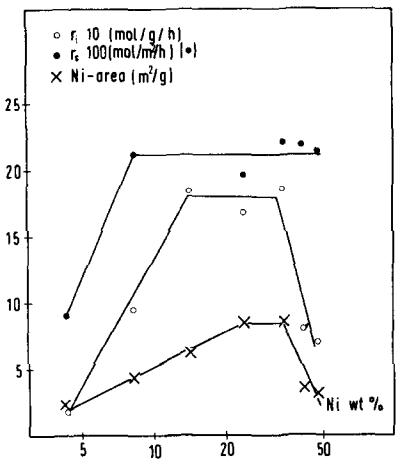

FIG. 4. Influence of Ni content on Ni surface area and activity for ethane reforming at 500°C. Catalysts A26–A32.

tassium is remarkable as sulfur poisoning of catalyst A1 involving a gradual blocking of the nickel surface is causing a decline of the specific activity by only approx 50%. This appears from Table 5 showing in addition an influence of other poisons such as chlorine and arsenic being less than that of potassium.

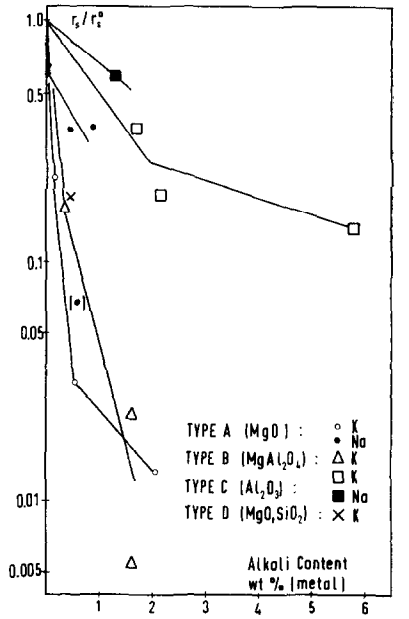

FIG. 5. Influence of alkali on the specific activity for ethane reforming at 500°C.

TABLE 5
THE INFLUENCE OF POISONS ON THE ACTIVITY OF CATALYST A1

Expt no.	Poison	Content (wt ppm)	Sulfur capacity (wt ppm)	Coverage	$r_i \times 10$ (g mol/g/hr)	$r_s \times 10^3$ (g mol/ m² Ni/hr)
Av of unpoisoned A1	—	80	883	<0.1	2.41	120
4201	S	239	805	0.30	0.66	62
4202	S	360	805	0.45	0.53	69
4203	S	398	805	0.49	0.59	64
329	S	615	805	0.76	0.38	56
55	S	805	805	1.00	<0.01	—
133	Cl	1350	885	?	2.43	
141	As	4200	885	?	0.55	

The presence of potassium implied no decrease of the nickel surface area determined by chemisorption of hydrogen sulfide at 550°C or as demonstrated previously (*15*) by chemisorption of hydrogen at −72°C. However, the measurements of nitrogen adsorption on the nickel surface shown in Tables 2 and 3 were significantly influenced by the addition of potassium. As, moreover, the nitrogen capacity of the zirconia-based catalyst D4 was negligible, it is natural to correlate catalyst activity and nitrogen capacity. This has been done in Fig. 6 and a correlation coefficient of 0.94 indicating great significance was calculated. Although the correlation reflects the great uncertainty of the adsorption measurements and does not account for the relatively low activity of the silica–alumina supported catalyst D9, it seems likely that the differences in specific activities are related to inhomogeneities of the nickel surface. It does not necessarily ascribe a special high activity to B_5-sites, as the number of these sites in some way is correlated with the number of other surface configurations such as corner atoms with low coordination numbers.

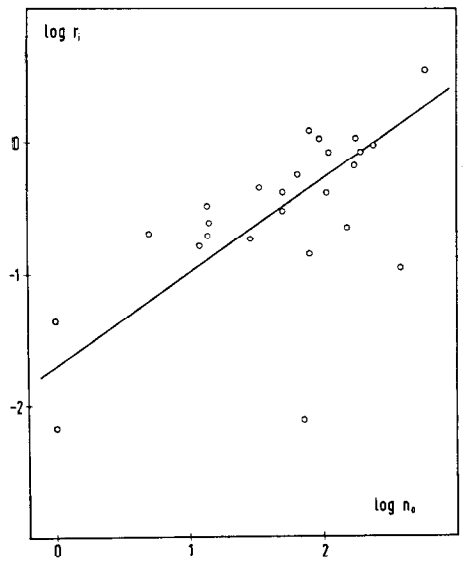

FIG. 6. N_2 capacity and activity for ethane reforming at 500°C.

Measurements on catalysts containing different metals showed large variations of specific activities. From Tables 2 and 3 the specific activities of metals based on alumina or magnesia may be listed as follows:

$$\text{Rh, Ru} > \text{Ni, Pd, Pt,} > \text{Re} > (Ni_{0.7}Cu_{1.3}) > \text{Co.}$$

The low activity of E10 could be explained by some irregularities in the preparation. The low activity of cobalt may be related to the process conditions with a H_2O/H_2 ratio close to the equilibrium constant for oxidation of cobalt by steam. The precious metals supported by carbon showed very poor activities similar to the results with carbon supported nickel catalysts.

2. Other Reactions at Atmospheric Pressure

In some reforming experiments with catalyst A1, ethane was replaced by methane or *n*-butane. First order kinetics were applied for methane reforming experiments. This was justified by an experiment show-

TABLE 6
REFORMING EXPERIMENTS AT ATMOSPHERIC PRESSURE VARIOUS HYDROCARBONS, CATALYST A1

Feed	Sp act (500°C)[a] × 10^3 r_s (mol/ m^2 hr)	r_{sc} (g atom/ m^2 hr)	App. activation energy[b] E_a (kcal/mol)
CH_4	61	61	26.2 (0.4)
C_2H_6	120	240	18.1 (0.15)
nC_4H_{10}	138	552	18.6 (0.6)

[a] Rates calculated for same partial pressure of hydrocarbon ($H_2O/C_nH_m = 8$; $H_2O/H_2 = 10$; 500°C).

[b] Figures in parentheses indicate the accuracy of E_a.

ing the kinetic coefficient to be close to unity. Equation (13) was used for evaluation of butane reforming experiments. The results are summarized in Table 6. The initial specific rates have been calculated at the same partial pressure of the hydrocarbon. The apparent activation energy is higher for methane than for ethane reforming, and a smaller reactivity is reflected by a lower initial specific rate. Contrary to this *n*-butane shows an activation energy and molar specific rate very close to that of ethane. This implies that the rate per carbon atom is higher for *n*-butane than for ethane. Moreover, it was observed that in the temperature range 400–525°C the reaction with *n*-butane resulted in no higher hydrocarbons among the products.

Results from experiments on hydrogenolysis of ethane and decomposition of ammonia are shown in Figs. 7 and 8, respectively. The trends of activities for these reactions, methane reforming and methanation of carbon monoxide were compared with the activity trend for ethane reforming by calculating activities relative to catalyst A1. The results are shown in Table 7.

The activity trends for ethane and methane reforming, ethane hydrogenolysis and methanation are broadly in line. Thus, the presence of potassium affects all these reactions by decreasing the specific activity. The data for methanation show some deviations from those for ethane reforming. Firstly, the catalysts based on zirconia (D4) and carbon (D14) show relatively high activities. Secondly, it appears that the specific activity of highly active catalysts, particularly those based on alumina, is higher than the corresponding values for ethane reforming. On the other hand, the influence of alkali appears to be more pronounced for methanation.

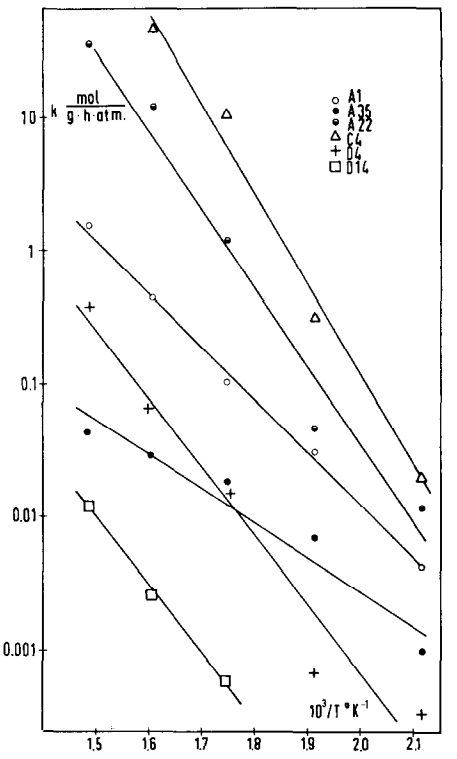

FIG. 7. Ethane hydrogenolysis. Temperature dependence of rate constants for various catalysts.

The results from decomposition of ammonia differ significantly from the general trend, as no decrease of the specific activity is observed for potassium-promoted catalysts and D4. No large changes of specific activities are observed, and as shown in Fig. 9 the activities for ammonia decomposition correlate simply with the nickel area. The cobalt-containing catalyst (A33) fits into this correlation.

3. Reforming Experiments at Pressure

The reforming experiments at pressure with 1–2 mm particles were subject to great

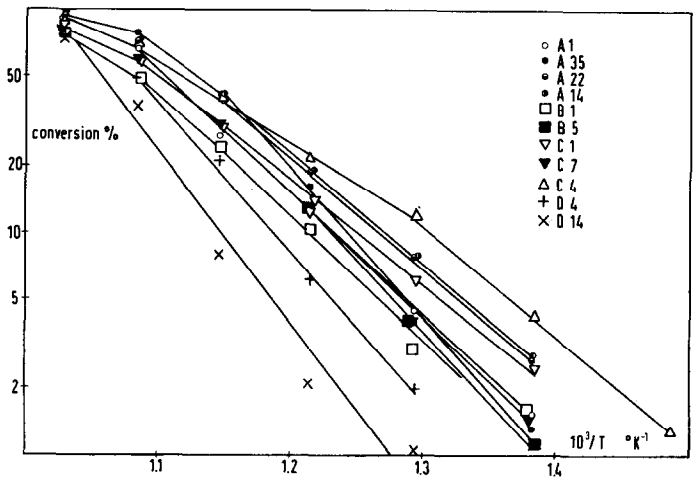

FIG. 8. Ammonia decomposition. Temperature dependence of conversion at standard conditions.

uncertainty as explained previously. This makes a more detailed evaluation doubtful. However, the results plotted in Fig. 10 show the conversion of ethane to increase with pressure. In principle, this could be explained by Knudsen diffusion causing severe restrictions at low pressure but the results from the experiment, 1231, performed at constant pressure and varying nitrogen flow indicates the pressure effect on the conversion to be related to the kinetics. When using naphtha as feed, positive and negative pressure effects are observed depending on the type of catalyst. As shown in Fig. 11 the conversion increases with pressure for catalysts A1 and B6, whereas the opposite effect is observed for the strongly alkalized B4. These results correlate with the kinetic coefficients for ethane reforming at atmospheric pressure listed in Table 4 which indicates the overall pressure coefficient to be positive for A1 and B6 and negative for B4.

The activities of various catalysts obtained by reforming of naphtha at 31 atm abs correlate with the corresponding activities determined by ethane reforming at atmospheric pressure. This is demonstrated in Fig. 12, where the straight line reflects the correlation for equal specific activities.

TABLE 7

RELATIVE SPECIFIC ACTIVITIES AT ATMOSPHERIC PRESSURE

Catalyst		Reforming		Hydrogenolysis of	Methanation of	Decomp. of
No.	Remarks	C_2H_6 500°C	CH_4 500°C	C_2H_6 300°C	CO 250°C	NH_3 500°C
A1	(0.07 wt % Na)	1.0	1.0	1.0	1.0	1.0
A22		2.4	2.0	4.2	9.1	0.9
A35	0.53% K	0.03	0.09	0.08	0.002	0.9
B1		3.0	1.4			3.2
B5	1.57% K	0.02	0.02			1.5
C1		0.7			2.7	0.4
C4		2.5		8.7	20.6	0.5
C7	5.8 wt % K	0.09			0.001	0.5
D4	ZrO_2	0.02	0.01	0.08	0.8	0.4
D8	SiO_2	1.1			4.9	
D9	SiO_2/Al_2O_3	0.2			0.04	
D14	Carbon	0.04	0.04	0.01	0.4	0.5

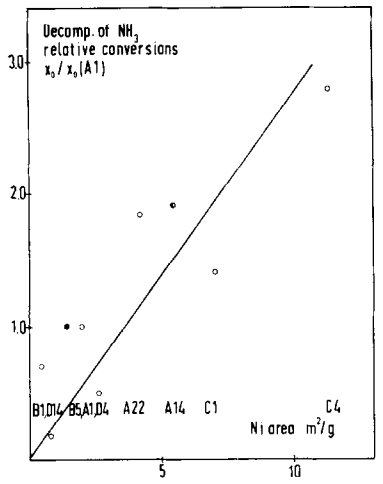

FIG. 9. Ammonia decomposition at 500°C. Activity as function of nickel surface area. Activity expressed as conversion at standard conditions relative to catalyst A1.

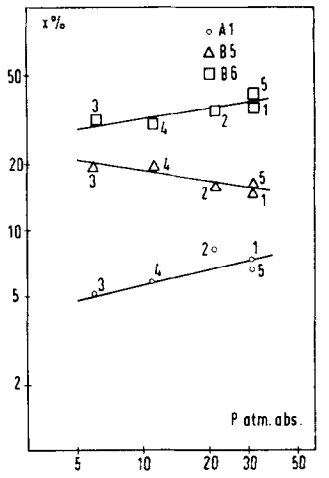

FIG. 11. Reforming of naphtha 36 at pressure. Pressure dependence of conversion at standard conditions at 500°C. Expt 1206: 0.5 g A1; Expt 1195: 10.7 g B5 (1.5 wt % K); Expt 1196: 11.7 g B6 (0.3 wt % K). Numbers indicate sequence of measurements.

Experiments with various hydrocarbons performed at 31 atm abs and 500°C using a fixed steam to carbon ratio revealed great differences in conversions. As shown in Table 8 most hydrocarbons are more reactive than is methane. Normal paraffins appear less reactive than isoparaffins and naphthenes whereas the reactivity of benzene is very close to that of methane. However, it should be noticed that the experiments are performed at a fixed steam to carbon ratio which implies that the partial pressure of the hydrocarbons varies with the number of carbon atoms of the hydrocarbon. As mentioned previously, extrapolation by means of the apparent rate constant k_a is very doubtful. When the con-

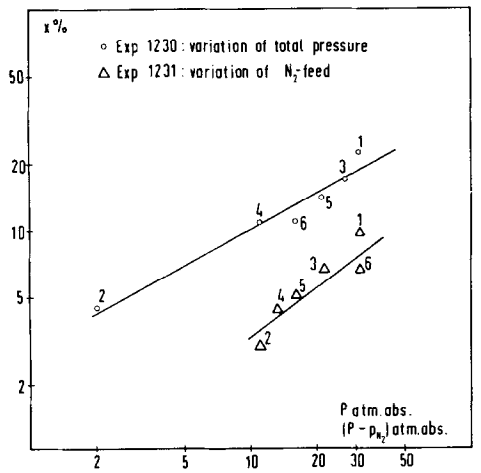

FIG. 10. Ethane reforming at pressure. Pressure dependence of conversion at standard conditions at 500°C. 0.5 g catalyst A18. The numbers indicate the sequence of measurements.

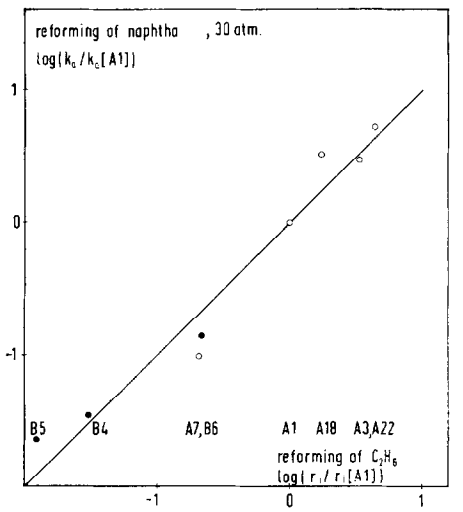

FIG. 12. Correlation between relative activities at 500°C for reforming of naphtha 36 at 30 atm and reforming of ethane at atmospheric pressure. Activities expressed relative to catalyst A1.

TABLE 8
REFORMING AT PRESSURE[a]

Exp. no.	Feed	H_2O/C (mol/atom)	$p_{C_nH_m}$ (atm)	Space velocity $\frac{\text{g atoms} \cdot 22.4}{\text{kg cat.}} \times 10^3$	Conversion to CO, CO_2, CH_4 (%)	k_a calc. from (13) (g atom/g/hr)	$k_a \times$ (no. C-atoms/ no. C–C bonds)	$k_a \times \frac{p_{CH_4}}{p_{C_nH_m}}$
1211	Methane	3.71	6.0	194	4.65[b]	0.43	—	0.43
1212	Ethane	3.79	3.3	207	31.5	3.5	1.8	6.4
1230		3.85	3.2	204	22.5	2.3	1.2	4.3
1216	(*n,iso*)Butane)	3.85	1.7	204	39.9	4.6	3.5	16
1210	Cyclohexane	3.73	1.2	209	53.9	7.2	7.2	36
1208	Benzene	3.96	1.1	200	5.7	0.53	0.53	2.9
1209	*n*-Heptane	3.83	1.0	206	18.7	1.9	1.6	11
1214	Trimethyl-butane	3.88	1.0	201	33.2	3.6	3.1	22
1213	*n*-Decane	3.77	0.7	104	32.8	1.9	1.7	16
1203	Naphtha 36 (FBP 120°C)	3.74	—	209	40.0	4.8	—	—
1215		3.76	—	209	35.8	4.1	—	—
1207	Naphtha 49 (FBP 169°C)	3.69	—	212	15.5	1.6	—	—

[a] Experiments with various hydrocarbons; Catalyst A18 (0.5 g as 1-2 mm particles); temp. 500°C; pressure 31 atm abs; $H_2O/H_2 = 10$.
[b] Conversion to CO and CO_2.

stants are corrected for the actual partial pressures of the hydrocarbons and assuming first order kinetics as shown in Table 8, the results indicate normal paraffins to be more reactive with increasing number of carbon atoms. This trend is still obtained when assuming a reaction order of 0.5 with respect to the hydrocarbon, and it is in accordance with the results obtained at low pressure shown in Table 5.

The analyses of higher hydrocarbons in the reactor effluent shown in Table 9 indicate the composition to be very close to that of the feedstock. This observation is in accordance with the result obtained in the reforming experiment with *n*-butane at atmospheric pressure. Therefore, the presence of intermediates in the products is very unlikely. The experiment with benzene represents an exception to this picture, and a detailed evaluation of the analysis of the unconverted naphtha from experiment 1207 appears very complicated.

Discussion

1. *Kinetics*

Although the kinetics of ethane reforming appear complex it may be helpful to discuss qualitatively the parameters involved in terms of a simple speculative sequence. Ethane is assumed to be chemisorbed on nickel following the pattern generally proposed in studies of ethane hydrogenolysis (*11*). An initial chemisorption step on a dual site involving dehydrogenation is followed by a rupture of the carbon–carbon bond and formation of a surface radical CH_x. Adsorption of steam on the carrier is assumed to be involved on the basis of the observed influence on the kinetic coefficient for water of the type of support material and of the presence of alkali. A rôle of the carrier for steam adsorption has also been suggested in the literature (*4, 6, 8*). When S_1 and S_2 are empty sites on the surface of nickel and the carrier respectively, the following sequence can be formulated:

$$C_2H_6 + 2S_1 = (S_1)_2\text{–}C_2H_z + \frac{6-z}{2}H_2, \quad (14)$$

$$(S_1)_2\text{–}C_2H_z + H_2 = 2S_1\text{–}CH_x, \quad (15)$$

$$H_2O + S_2 = S_2\text{–}H_2O, \quad (16)$$

$$S_2\text{–}H_2O + S_1 = S_1\text{–}O + H_2S_2, \quad (17)$$

$$S_1\text{–}CH_x + S_1\text{–}O = 2S_1 + CO + \frac{x}{2}H_2, \quad (18)$$

$$CO + S_1\text{–}O = S_1 + CO_2. \quad (19)$$

Certainly, steps (14) and (15) represent a simplification because there may be a gradual formation of strongly adsorbed species by further dehydrogenation. As discussed by Kemball (*27*) and Frennet and Lienard (*28*) these species may become less reactive and may therefore diminish the surface available for the reaction. Eventually they may be converted to carbon.

For ethane hydrogenolysis the rupture of the carbon–carbon bond is generally assumed to be the rate determining step of the overall reaction, all other steps being in quasi-equilibrium (*11, 29, 30*). In other studies (*31–33*) it is believed that the desorption of products is rate determining. Recently Boudart (*34*) has considered the reaction as two irreversible steps.

These opposite views are reflected by the assumptions made in the formulation of kinetics for reforming reactions. Balashova, Slovokhotova and Balandin (*4*) argued for the rupture of the carbon–carbon bond as the rate determining step, whereas Bhatta and Dixon (*5*) and Saito *et al.* (*8*) were in favor of the desorption of products or the reaction with steam being the slow step. Phillips, Mulhall and Turner (*7*) suggested that the rate determining step varies with the type of hydrocarbon, whereas Bodrov, Apel'baum and Temkin (*9*) for methane reforming assumed the reaction with steam to be rate determining at low temperature and the chemisorption of methane to be limiting at high temperature.

There are some objections to discussing the kinetics by means of a single rate determining step. Firstly, as proposed by Boudart (*34*), the dissociative chemisorption of ethane is most probably irreversible in the temperature range of the present study. Secondly, for practical purposes, the surface reaction (18) might also be considered as irreversible since no influence on the

TABLE 9

REFORMING EXPERIMENTS WITH VARIOUS HYDROCARBONS[a]

Expt no.:	1216 Butane		1210 Cyclohexane		1208 Benzene		1209 *n*-Heptane		1214	1213	1215 1203	1207 Naphtha 49[d]	
Feed: Analyses (wt %)	Feed[b]	Liq. prod.[c]	Feed	Liq. prod.	Feed	Liq. prod.	Feed	Liq. prod.	Tri meth. buta. Feed	*n*-Decane Feed	Naphtha 36[d] Feed	Feed	Liq. prod.
C_2H_4	0.01	0.04											
C_2H_6	0.05	0.47										0.10	
$C_3H_8 + (C_3H_6)$	1.20	1.57										1.13	
n-C_4	80.30	79.00									0.02	3.70	
i-C_4	17.92	18.61										1.08	
C_4H_8	0.27	0.00							0.05				
n-C_5	0.25	0.31			0.01	0.01	0.06	0.02	0.32		29.16	3.92	2.05
i-C_5							0.01		0.11		8.55	4.45	0.22
CP											1.74	0.51	0.22
n-C_6				1.65	0.01	0.08	0.82	0.57			16.51	4.39	4.51
i-C_6				0.02		0.04	0.06	0.04			16.84	4.70	3.58
MCP(+22DMP)				0.92	0.04	0.03	0.17	0.10			3.40	2.72	1.20
CH(+33DMP)			99.98	96.34	0.07	0.06	0.47	0.36	0.06		1.86	1.80	1.19
Benzene					99.71	62.23	0.05	0.24	0.56		1.24	0.23	0.39

n-C_7	0.01	0.72	0.02	0.38	86.40	87.71	0.01		5.14	5.21	7.02
iso-C_7		0.18	0.07	0.17	8.45	7.67	98.78		5.45	4.78	5.50
DMCP		0.01		0.11	1.72	1.52			1.53	4.31	3.06
MCH(+22DMH + 113TMCP)	0.01	0.06		0.35	0.72	0.69			1.72	6.66	5.49
ECP(+25DMH)		0.01		0.11	0.19	0.18			0.52	1.04	1.15
Toluene		0.03		0.38	0.37	0.36			1.76	1.82	2.70
n-C_8				3.26	0.31	0.35			1.02	6.40	7.16
iso-C_8 + C_{8+}		0.06	0.07	3.30	0.20	0.19			2.33	11.87	14.60
ECH				0.82					0.09	2.53	1.74
Ethylbenz				0.54					0.12	0.30	1.10
Xylenes				3.00					0.33	4.36	4.48
n-C_9				5.06					0.37	4.60	5.02
C_{9+}				10.26					0.17	10.43	15.41
n-C_{10}				1.61				>95	0.06	0.18	1.43
C_{10+}				7.02					0.07	2.07	9.62
n-C_{11}				0.09							0.06
C_{11+}				1.09							1.10

[a] Temp: 500°C; pressure: 30 atm abs; catalyst: A18; gas chromatographical analyses of feed and liquid products.
[b] CH_4: 0.01 vol %.
[c] Calculated from gas analysis.

[d] Naphtha no.:	36			49		
ASTM: IBP/MBP/FBP (°C)	40	65	120	40	89	169
Spec gr (g/ml)		0.674			0.705	

rate of carbon dioxide was indicated. Moreover, the surface species S_1–CH_x and probably also S_1–O may be assumed to be the most abundant surface intermediates, the concentrations of other intermediates being negligible. There is some evidence for this assumption. As no intermediates are found in the products when using *n*-butane or higher hydrocarbons (except benzene) as feed, this may indicate the same active species, containing one carbon atom, to be involved in the reaction. In addition, some LEED studies by Maire *et al.* (*35*, *36*) have shown similar structures of the type CH_x to be formed by adsorption on nickel of methane, ethane, propane and neopentane.

These assumptions lead to the following equations for the rates of the steps and for the total number of sites, L and M, on the surface of nickel and carrier, respectively:

$$r_{14} = r_{15} = \tfrac{1}{2}r_{18} \quad r_{+16} = r_{-16} \quad r_{+17} = r_{-17},$$

$$(S_1) + (S_1\text{–}CH_x) + (S_1\text{–}O) = L,$$

$$(S_2) + (S_2\text{–}H_2O) = M, \quad (20)$$

the remaining steps involved in establishment of the equilibria (2) and (3) being kinetically insignificant in accordance with the principle formulated by Boudart (*34*). Using Langmuir equations and thus assuming a homogeneous surface and no changes of heats of adsorption with coverage the following rate equation is obtained:

$$r = \frac{k_A L^2 \cdot p_{C_2H_6}}{[(1 + (2k_A/k_r)\,(1/K_w)(p_{C_2H6}/p_{H_2O})p_{H_2} + K_w(p_{H_2O}/p_{H_2})]^2}, \quad (21)$$

where $k_A = k_{14}$, $k_r = k_{18}$ and $k_w = k_{+16} \cdot k_{+17}/(k_{-16} \cdot k_{-17})$.

From this expression it is possible qualitatively to comprehend the varying kinetic coefficients reported in the literature (Table 1) and observed in this study (Table 4). The kinetic order with respect to steam may become positive or negative depending on the size of the equilibrium constant for steam adsorption, K_w, and the relative sizes of the rate constants for the hydrocarbon adsorption, k_A, and the surface reaction, k_r. Since K_w is the product of the equilibrium constants of steps (16) and (17) it is strongly influenced by the adsorption properties of the carrier material. A possible temperature dependence of reaction orders is clear since the relative size of the terms of denominator may change with temperature depending on the sizes of the activation energies for the hydrocarbon adsorption and the surface reaction, and the heat of adsorption for steam. The different reactivities of various hydrocarbons may be reflected by the size of k_A, which may also be affected by the presence of some optimal sites on the nickel surface. Surface heterogeneities were ignored in the derivation of (21) but as demonstrated by Boudart (*34*, *37*) this will still lead to rate functions being qualitatively correct. If step (15) is assumed to be rate determining the second term of the denominator in (21) disappears. An expression of that form was derived by Lička (*38*).

Equation (21) may be converted to a power-rate law using the well-known approximation of the term $ax/(1 + ax)$ by the term bx^a where $0 < \alpha < 1$:

$$r = k_n p_{C_2H_6}{}^{1-2m} \cdot p_{H_2O}{}^{2(n-m)} p_{H_2}{}^{2(m-n)}, \quad (22)$$

where $0 < m < 1$, and $0 < n < 1$.

This expression may explain the kinetic coefficients obtained for catalyst A1 as shown in (13), and that the kinetic coefficient for steam may become less than -1 as observed for catalysts A35 and B4, but the reaction orders with respect to steam and hydrogen are not numerically equal as predicted.

In addition, the overall pressure coefficients to be deduced from Fig. 11 correlate with the kinetic order for steam indicating the rôle of hydrogen to be more complicated than accounted for in the simple sequence.

In Boudart's (*34*) recent kinetic interpretation of ethane hydrogenolysis hydrogen is assumed to be in a chemisorption equilibrium with nearby saturated sites on the metal surface different from the sites where the hydrocarbon reacts. If so, step (14)

should be reformulated by:

$$H_2 + 2S_3 = 2(S_3)\text{–}H, \quad (23)$$

$$C_2H_6 + 2S_1 + yS_3 = (S_1)_2\text{–}C_2H_z + y(S_3)\text{–}H + \frac{6 - y - z}{2} H_2. \quad (24)$$

This implies that the term $p_{C_2H_6}$ in (21) and (22) should be replaced by $p_{C_2H_6}/p_{H_2}^{y/2}$. Hence:

$$r = \frac{k'_A(p_{C_2H_6}/p_{H_2}^{y/2})}{[1 + (2k'_A/k_r)(1/K_w) \cdot (p_{C_2H_6}/p_{H_2O}) \cdot p_{H_2}^{1-(y/2)} + K_w(p_{H_2O}/p_H)_2]^2}, \quad (25)$$

$$r = kp_{C_2H_6}^{1-2n} \cdot p_{H_2O}^{2(n-m)} \cdot p_{H_2}^{2(m-n)-(n/2)y}. \quad (26)$$

The simple sequence for hydrocarbon adsorption simulating the steps suggested in hydrogenolysis remains speculative, and it may hardly be used for evaluation of the reactivity trend of the higher hydrocarbons because the results from hydrogenolysis have been reported mainly for temperatures below 400°C.

The apparent multiple fission of carbon–carbon bonds and the relatively high reactivity of branched hydrocarbons and cyclohexane deviates from the pattern generally observed in hydrogenolysis at low temperature, nickel attacking selectively the ends of chains (*39*). However, in reforming studies in the temperature range 250–350°C Balashova, Slovokhotova and Balandin (*40*) found a stepwise degradation of hydrocarbons and a much higher reactivity of *n*-paraffins than of cycloparaffins. At higher temperatures, 350–450°C, Phillips, Mulhall and Turner (*7*) observed partially decomposed hydrocarbons from the reforming reaction with branched hydrocarbons which were less reactive than normal paraffins. Methyl cyclohexane was found to be slightly less reactive than normal heptane and a small amount of toluene was found among the products. In the present study at 500°C intermediates were indicated only for benzene this being the least reactive hydrocarbon. In experiments at very high temperatures 750–950°C, Yoshitomi, Morita and Yamamoto (*41*) found cyclohexane to be more reactive than *n*-hexane above approx 800°C. Although thermal pyrolysis must have influenced the latter results, the relative reactivities appear to vary with temperature. This conclusion is supported by the different activation energies for normal and cycloparaffins reported by Balashova, Slovokhotova and Balandin (*40*).

At 600°C Schnell (*42*) was able to detect substantial amounts of low olefins in reforming experiments with propane and butane performed at very short contact times. In the present experiments on butane reforming at atmospheric pressure conversions and contact times (approx 2×10^{-3} sec) were within the range considered by Schnell. Since no intermediates were identified in these studies performed at 400–525°C, the olefins observed by Schnell are most probably not intermediates from the reaction on the nickel surface but products from thermal pyrolysis or cracking on the carrier material, these reactions being more pronounced at the temperature level applied by Schnell. On this basis, it appears reasonable to assume multiple fission of the carbon–carbon bonds on the nickel surface for most nonaromatic hydrocarbons at temperatures of 500°C and above, and to consider minor amounts of ethane, propane and other higher hydrocarbons which might be observed in the effluent of some tubular reformers as being hydrogenated products from pyrolysis or cracking.

2. *Catalyst Activity*

The results shown in Table 7 demonstrated that the specific activity of nickel for reforming reactions, hydrogenolysis and methanation is strongly influenced by the carrier employed and by the presence of alkali. A parallelism of activity trends is observed. Another common feature of these reactions is a resemblance of the trend of specific activities of different metals, ruthenium and rhodium being reported to show much higher specific activities for hydrogenolysis (*11*) and methana-

tion (*43*) than do nickel, platinum, and palladium. Contrary to this, ammonia decomposition appears unaffected by the carrier and the presence of alkali. This makes doubtful the use of this reaction for activity tests of reforming catalysts as proposed by Merkel (*44*).

A carrier effect in reforming reactions has also been described by Balashova, Slovokhotova and Balandin (*4*) who found nickel on carbon to be nearly inactive for reforming of cyclohexane compared with nickel on silica. Balashova, Slovokhotova and Balandin explained the difference by a failing ability of coke for activation of steam since the two catalysts showed comparable activities for dehydrogenation of cyclohexane. However, as proven by the hydrogenolysis experiments, nickel on carbon may show poor activity in other reactions where steam is not involved.

A low activity for hydrogenolysis has also been reported by Sinfelt (*11*) for cobalt on carbon. Moreover, Sinfelt showed the specific activity for hydrogenolysis of silica–alumina-based nickel catalysts to be much less than those of alumina- or silica-based catalysts, the latter being the most effective. These results are in accordance with the trend observed for ethane reforming in the present study, although the accuracy of the experiments does not allow a distinction between alumina- and silica-based catalysts. For methanation of carbon dioxide Pour (*45*) found the specific activity of supported nickel to decrease in the order chromia, alumina, silica.

The diminution of the activity for reforming reactions caused by alkali was mentioned by Andrew (*3*). The effect was explained by adsorption of alkali blocking the most active sites on the nickel surface. When this explanation is applied for the present measuements, it implies that the adsorption of alkali is not affecting the sites for ammonia decomposition. Moreover, it implies that alkali is adsorbed more specifically at the most active sites than is sulfur, because as mentioned earlier, the specific activity displays a more drastic fall by increasing the amount of alkali than by increasing the amount of sulfur. This behavior appears unlikely but, in principle, it cannot be excluded, as demonstrated by Roginskii (*46*).

The effect of alkali has also been reported for hydrogenolysis. Cimino, Boudart and Taylor (*47*) observed a great effect of alkali on the kinetics of ethane hydrogenolysis on iron. This effect was explained by assuming alkali to depress the affinity of the surface for hydrogen so that dehydrogenation of the adsorbed hydrocarbon is retarded. In the simple sequence (14) this means a higher value of z. Shephard (*33*) observed a similar effect on a nickel alumina catalyst and noticed that removal of alkali resulted in increased specific activity. For methanation of carbon monoxide Schoubye (*12*) reported low activities of alkali-promoted catalysts.

The evaluation of interactions between metal and support has been an intricate subject of catalysis. Bifunctional catalysis is not very likely to be involved apart from the rôle of the carrier in steam adsorption which cannot explain the different specific activities. As discussed earlier, cracking on the carrier surface may be excluded in the temperature range applied in the experiments and no correlation between surface acidity and specific activity is apparent. Thus catalysts based on magnesia, spinel and γ-alumina show specific activities within the same range. A similar conclusion on a rôle of acid sites for hydrogenolysis was arrived at by Richardson (*48*).

The electronic nature of the support was emphasized in the work by Schwab *et al.* (*49*) and Szabo and Solymosi (*50*). A change of the activation energy with the doping of oxides supporting thin nickel films was assigned to a change of the semiconductor properties of the carrier influencing the Fermi level of the electrons of the metal phase. However, from later developments (*51*) there is much evidence for the localized chemical properties of the surface atoms being important for the catalytic reaction rather than the collective properties of the bulk phase. Therefore, apart from extremely small metal crystallites as used by Dalla Betta and Boudart (*52*) an electronic interaction between the carrier

and the surface atoms of the metal is very unlikely. The measurements reported in Table 4 and Fig. 3 are in accordance with this statement, as the use of zirconia (D4) or the presence of alkali (A34 and A35) resulting in low specific activities are accompanied by no detectable change of the activation energies. Contrary to this, an increased activation energy observed when using a nickel–copper catalyst (A13) may be explained by an influence on the nickel surface atoms of neighboring copper atoms.

As mentioned earlier the correlation shown in Fig. 6 indicates that different specific activities might be related to the heterogeneity of the nickel surface which presumably is influenced by the carrier. The reforming reactions, hydrogenolysis and methanation may therefore be characterized as structure-sensitive, while decomposition of ammonia appears "facile". The effect of surface structure is often studied on a series of catalysts with varying metal crystallite size because heterogeneity of the surface is expected to increase by decreasing the crystallite size in the range below approx 70 Å (*17*). In hydrogenolysis results appear ambiguous, as Sinfelt (*11*) found an effect for nickel on silica–alumina, whereas the activity showed no variation with crystallite size for nickel on silica. For methanation on nickel supported by alumina Bousquet and Teichner (*53*) found no influence on the specific activity of crystallite size. The nickel crystallites of the catalysts in the present study are nearly all outside the range of interest, and reforming of ethane appears to be unaffected by the crystallite size as shown in Fig. 4, although a decrease of the specific activity with crystallite size might be indicated for the catalyst with the smallest crystallites.

Meanwhile, surface heterogeneity is not only a result of crystallite size but rather a matter of surface topography, with the existence of ensembles of nickel atoms on the surface being optimal for the particular reaction in question. The configuration of such ensembles may vary from reaction to reaction. Thus, Ponec and Sachtler (*54*) from their work on nickel–copper alloys suggested that the ensembles required for reactions affecting the carbon–hydrogen bond or leading to isomerization contain a smaller number of adjacent nickel atoms than the ensembles required for hydrogenolytic splitting of the carbon–carbon bond.

On larger crystals the number of special ensembles may vary with crystal orientation (*55*, *56*) or the ensembles may be related to epitaxial relations or abnormal shapes of the crystals which could be stabilized by the support material. The interface is extremely complex as chemical reactions may be involved. In principle, the shape of the metal particle is influenced by the anisotropy of the surface energy of the metal and by the interfacial energy (*57*). Unfortunately, very few studies have been reported on this effect. For liquid nickel droplets at 1500°C Kingery (*58*, *59*) found a significantly higher adhesion energy and correspondingly low interfacial energy and contact angle for stabilized zirconia as support than for alumina. Studies *in vacuo* of nickel droplets on various materials indicated by low contact angles that wetting was more pronounced on graphite than on several oxides. Contact angles on zirconia and titania were lower than on magnesia, alumina and beryllia. Preferential adsorption of impurities at the interface may lower the interfacial energy and result in facetting and other equilibrated shapes (*58*, *60*, *61*).

It is evident that these observations allow no conclusions to be made concerning the effect of the carrier on the catalytic activity of the metal. In addition, use of data obtained for droplets at high temperature appears doubtful. However, there may be some indication that carrier materials showing high adhesion energy and thus influencing the shape of the metal particle cause a decrease of the number of ensembles for the reforming reactions. Moreover, it is conceivable that the influence of alkali is caused by adsorption of alkali at the interface or on the metal changing the shape of the crystal or the facetting of the planes. Shephard (*33*) also considered the importance of various crystallite forms for the activity for hydrogenolysis. Exami-

nation in the electron microscope of the catalysts of this study revealed no marked differences between active and poor catalysts, and more detailed studies on well-defined systems are required to evaluate these effects.

Conclusions

The kinetics and the specific activity for reforming reactions vary from catalyst to catalyst. The major differences in the kinetics are found in the influence of steam partial pressure. This is related to the ability of the carrier material to adsorb steam. Active magnesia or the presence of alkali enhance steam adsorption. The kinetics cannot be described in a broad temperature range by a simple power law, as the powers vary with temperature.

At temperatures around 500°C the results indicate multiple fission on the nickel surface of the carbon–carbon bonds for most nonaromatic hydrocarbons. The reactivity of normal paraffins at equal partial pressures appears to increase with the number of carbon atoms. The reactivity of branched hydrocarbons and cycloparaffins appear higher than those of normal paraffins whereas aromatics show poor reactivity.

The activities per unit nickel surface area, the specific activities, are within the same range for a great number of catalysts irrespective of the nickel surface area, support material, preparation or activation procedure. Use of supports such as zirconia and carbon results in very poor specific activities, whereas some decrease of the specific activity is observed when using silica–alumina and titania. Addition of alkali in various ways implies a significant drop in specific activity, the effect of potassium being larger than for sodium.

The activity trends observed for reforming reactions are generally in accordance with results obtained or reported for ethane hydrogenolysis and methanation, whereas the specific activity for decomposition of ammonia appears unaffected by the carrier and the presence of alkali. It is unlikely that this effect of the carrier and alkali is related to the ability for steam adsorption or to surface acidity. Morever, electronic interactions between carrier or alkali and the metal may be excluded, since the effect is not accompanied by a change of the activation energy.

The results indicate that the activity for reforming correlates with the surface heterogeneity as expressed by the adsorption of nitrogen on the nickel surface. It is believed that some carrier materials and adsorption of alkali on the interface or the metal may influence the surface structure by changes of the surface and interfacial energies. This might affect the number of ensembles being optimal for reforming reactions, hydrogenolysis and methanation.

Acknowledgments

The author thanks Dr. Haldor Topsøe for encouraging this work and his permission to publish the results. Thanks are given to Mrs. G. Parthum, Mr. J. Holst, Mr. C. Thomsen, Mr. P. Tøttrup, and many colleagues for assistance in performing the experiments. Mr. J. E. Jarvan has kindly assisted in preparing the computer calculations.

References

1. Rostrup-Nielsen, J. R., *Chem. Eng. Progr. Ammonia Safety Symp. Tech. Man.* **15,** (1973) in press.
2. Bridger, G. W., and Wyrwas, W., *Chem. Proc. Eng.* **48,** 101 (1967).
3. Andrew, S. P. S., *Ind. Eng. Chem., Prod. Res. Develop.* **8,** 321 (1969).
4. Balashova, S. A., Slovokhotova, T. A., and Balandin, A. A., *Kinet. Katal.* **7,** 303 (1966).
5. Bhatta, K. S. M., and Dixon, G. M., *Trans. Faraday Soc.* **63,** 2217 (1967).
6. Bhatta, K. S. M., and Dixon, G. M., *Ind. Eng. Chem., Prod. Res. Develop.* **8,** 324 (1969).
7. Phillips, T. R., Mulhall, J., and Turner, G. E., *J. Catal.* **15,** 233 (1969).
8. Saito, M., Tokuno, M., Ichiro, A., and Morita, Y., *Kogyo Kagaku Zasshi* **73,** 2405 (1970).
9. Bodrov, I. M., Apel'baum, L. O., and Temkin, M. I., *Kinet. Katal.* **9,** 1065 (1968).
10. Ross, J. R. H., and Steel, M. C. F., *J. Chem. Soc. Faraday Trans. 1* **69,** 101 (1973).
11. Sinfelt, J. H., *Catal. Rev.* **3,** 175 (1969).
12. Schoubye, P., *J. Catal.* **14,** 238 (1969).
13. Hougen, O. A., and Watson, K. M., "Chemical Process Principles," Part 3, p. 964. Wiley, New York, 1959.

14. ROSTRUP-NIELSEN, J. R., *J. Catal.* **27,** 343 (1972).

15. ROSTRUP-NIELSEN, J. R., *J. Catal.* **11,** 220 (1968).

16. VAN HARDEVELD, R., AND VAN MONTFOORT, A., *Surface Sci.* **4,** 396 (1966).

17. VAN HARDEVELD, R., AND HARTOG, F., *Surface Sci.* **15,** 189 (1969).

18. VAN HARDEVELD, R., AND HARTOG, F., *Proc. Int. Congr. Catal., 4th,* Moscow 1968, pap. 70; p. 295. Akademiai Kiado, Budapest, 1971.

19. VAN HARDEVELD, R., AND VAN MONTFOORT, A., *Surface Sci.* **17,** 90 (1969).

20. EISCHENS, R. P., AND JACKNOW, J., *Proc. Int. Congr. Catal., 3rd, 1964* **1,** 641 (1965).

21. KING, D. A., *Surface Sci.* **9,** 375 (1968).

22. ROEV, L. M., BATYCHKO, S. V., AND RUSOV, M. T., *Kinet. Katal.* **12,** 1072 (1971).

23. BRADSHAW, A. M., AND PRITCHARD, J., *Surface Sci.* **19,** 198 (1970).

24. BRADSHAW, A. M., AND PRITCHARD, J., *Surface Sci.* **17,** 371 (1969).

25. VAN HARDEVELD, R., private communication.

26. KJÆR, J., "Computer Methods in Catalytic Reactor Calculations," Vedbæk, 1972.

27. KEMBALL, C., *Discuss. Faraday Soc.* **41,** 190 (1966).

28. FRENNET, A., AND LIENARD, G., *Surface Sci.* **18,** 80 (1969).

29. BALANDIN A. A., SLOVOKHOTOVA, T. A., SHOLIN, A. F., AND UGOL'TSEVA, L. A., *Kinet. Katal.* **6,** 115 (1965).

30. GUCZI, L., GUDKOV, B. S., AND TÉTÉNYI, P., *J. Catal.* **24,** 187 (1972).

31. ANDERSON, J. R., AND BAKER, B. G., *Proc. Roy. Soc., Ser A* **271,** 402 (1963).

32. FREEL, J., AND GALWEY, A. K., *J. Catal.* **10,** 277 (1968).

33. SHEPHARD, F. E., *J. Catal.* **14,** 148 (1969).

34. BOUDART, M., *AIChE J.* **18,** 465 (1972).

35. MAIRE, G., ANDERSON, J. R., AND JOHNSON, B. B., *Proc. Roy. Soc., Ser. A* **320,** 227 (1970).

36. MAIRE, G., AND LEGARE, P., *J. Chim. Phys. Physicochim. Biol.* **68,** 1206 (1971).

37. BOUDART, M., *AIChE J.* **2,** 62 (1956).

38. LIČKA, S., thesis, Vyscká škola Chemicko-Technologická Praha, 1971.

39. MYERS, C. G., AND MUNNS, G. W., JR., *Ind. Eng. Chem.* **50,** 1727 (1958).

40. BALASHOVA, S. A., SLOVOKHOTOVA, T. A., AND BALANDIN, A. A., *Izv. Akad. Nauk SSSR Ser. Khim.* **2,** 275 (1965).

41. YOSHITOMI, S., MORITA, Y., AND YAMAMOTO, K., *Bull. Jap. Petrol. Inst.* **4,** 15 (1962).

42. SCHNELL, C. R., *J. Chem. Soc.* (B) 158 (1970).

43. MCKEE, D. W., *J. Catal.* **8,** 240 (1967).

44. MERKEL, H., *Brennst.-Chem.* **48,** 131 (1967).

45. POUR, V., *Collect. Czech. Chem. Commun.* **35,** 2203 (1970).

46. ROGINSKII, S. S., "Adsorption und Katalyse an inhomogenen Oberflächen," p. 17. Akademie Verlag Berlin, 1958.

47. CIMINO, A., BOUDART, M., AND TAYLOR, H., *J. Phys. Chem.* **58,** 796 (1954).

48. RICHARDSON, J. T., *J. Catal.* **21,** 122 (1971).

49. SCHWAB, G.-M., BLOCK, J., MÜLLER, W., AND SCHULTZE, D., *Naturwissenschaften* **44,** 582 (1957).

50. SZABO, Z. G., AND SOLYMOSI, F., *Actes Congr. Int. Catal.,* **2,** 1627 (1961).

51. SACHTLER, W. H. M., AND VAN DER PLANK, P., *Surface Sci.* **18,** 62 (1969).

52. DALLA BETTA R. A., AND BOUDART, M., *Proc. Int. Congr. Catal., 5th,* Palm Beach, FL, 1972, **2,** 1329 (1973).

53. BOUSQUET, J. L., AND TEICHNER, S. J., *Bull. Soc. Chim. Fr.* **10,** 3687 (1972).

54. PONEC, V., AND SACHTLER, W. H. M., *Proc. Int. Congr. Catal., 5th,* Palm Beach, FL, 1972, **1,** 645 (1973).

55. ANDERSON, J. R., MACDONALD, R. J., AND SHIMOYAMA, Y., *J. Catal.* **20,** 147 (1971).

56. CUNNINGHAM, R. E., AND GWATHMEY, A. T., *in* "Advances in Catalysis" (D. D. Eley, W. G. Frankenburg, V. I. Komarewsky, and P. B. Weisz, Eds.), Vol. 9, p. 25. Academic Press, New York, 1957.

57. WINTERBOTTOM, W. I., *Acta Met.* **15,** 303 (1937).

58. KINGERY, W. D., *J. Amer. Ceram. Soc.* **37,** 42 (1954).

59. HUMENIK, M., JR., AND KINGERY, W. D., *J. Amer. Ceram. Soc.* **37,** 18 (1954).

60. SUNDQUIST, B. E., *Acta Met.* **12,** 67 (1964).

61. ARMSTRONG, W. M., CHAKLADER, A. C. D., AND CLARKE, J. F., *J. Amer. Ceram. Soc.* **45,** 115 (1962).